Constraints on primordial black holes as dark matter candidates from star formation

Fabio Capela, Maxim Pshirkov, and Peter Tinyakov

Constraints on Primordial Black Holes as Dark Matter Candidates from Star Formation

Fabio Capela,[1] Maxim Pshirkov,[2, 3, 4] and Peter Tinyakov[1]

[1]Service de Physique Théorique, Université Libre de Bruxelles (ULB),
CP225 Boulevard du Triomphe, B-1050 Bruxelles, Belgium
[2]Sternberg Astronomical Institute, Lomonosov Moscow State University,
Universitetsky prospekt 13, 119992, Moscow, Russia
[3]Pushchino Radio Astronomy Observatory, Astro Space Center,
Lebedev Physical Institute Russian Academy of Sciences, 142290 Pushchino, Russia
[4]Institute for Nuclear Research of the Russian Academy of Sciences, 117312, Moscow, Russia

By considering adiabatic contraction of the dark matter (DM) during the star formation, we estimate the amount of DM trapped in stars at their birth. If the DM consists partly of primordial black holes (PBHs), they will be trapped together with the rest of the DM and will be finally inherited by a star compact remnant — a white dwarf (WD) or a neutron star (NS), which they will destroy in a short time. Observations of WDs and NSs thus impose constraints on the abundance of PBH. We show that the best constraints come from WDs and NSs in globular clusters which exclude the DM consisting entirely of PBH in the mass range 10^{16}g $- 3 \times 10^{22}$g, the strongest constraint on the fraction $\Omega_{\rm PBH}/\Omega_{\rm DM} \lesssim 10^{-2}$ being in the range of PBH masses 10^{17}g $- 10^{18}$ g.

PACS numbers:

I. INTRODUCTION

Various observational evidences point at the existence of a new matter component in the Universe, the dark matter (DM) (for a recent review see, e.g., [1, 2]). Observations of the cosmic microwave background imply that DM comprises $\sim 23\%$ of the total energy budget of the Universe, thus dominating in the matter sector, where baryonic component sums up to only 4% [3]. However, the nature of DM remains unknown and masses of possible candidates range over many orders of magnitude from a fraction of eV to many solar masses. Although most popular candidates are new stable particles, other possibilities are not excluded.

In the Early Universe density perturbations with high initial amplitude could collapse forming black holes [4]. If some of these black holes survive until now they could constitute (at least) a fraction of DM. Properties of these primordial black holes (PBHs) make them a suitable DM candidate: they are nonrelativistic and have subatomic size $r \sim 10^{-8}$ cm $(m_{\rm BH}/10^{20}g)$ which makes them effectively collisionless. Unlike most of other DM candidates, PBHs do not require the existence of new particle species.

The initial mass function of PBHs is flat in the case of a flat power spectrum of primordial density fluctuations. However, models with strongly non-flat mass function of PBHs can be constructed, see, e.g., Refs. [5, 6]. The constraints at different masses, therefore, should be considered independently.

The PBHs with masses $m_{\rm BH} \leq 5 \times 10^{14}$ g have lifetimes due to Hawking evaporation [7] shorter than the present age of the Universe. Such PBHs thus cannot contribute to the DM.

PBHs with slightly larger masses emit $\gamma-$rays with energies around ~ 100 MeV [8]. Observations of the extragalactic gamma-ray background with the Energetic Gamma Ray Experiment Telescope (EGRET) [9] set an upper limit on the cosmological density $\Omega_{\rm PBH}$ of such PBHs as a function of their mass, e.g. $\Omega_{\rm PBH} \leq 10^{-9}$ for $m_{\rm BH} = 10^{15}$ g [10]. These observations show that PBHs with masses $m_{\rm BH} \leq 10^{16}$ g can not constitute more than 1% of DM. However, the constraints coming from the process of Hawking evaporation disappear for PBH masses larger than $m_{\rm BH} \gtrsim 7 \times 10^{16}$ g.

The PBHs in the mass range $m_{\rm BH} \lesssim 10^{19} - 10^{20}$ g can be constrained with the so-called "femto-lensing" of the gamma-ray bursts [11]. Present day observations of gamma-ray bursts constrain the mass fraction of PBHs in the narrow mass range around $m_{\rm BH} \sim 10^{18}$ g at several percent level [12]. The abundance of more massive PBHs can be constrained from microlensing surveys. The EROS microlensing survey sets an upper limit of 8% on the fraction of the Galactic halo mass in the form of PBHs with masses in the range of 10^{26} g $< m_{\rm BH} < 3 \times 10^{34}$ g [13]. At even higher mass scales, 10^{33} g $< m_{\rm BH} < 10^{40}$ g, the analysis of the Cosmic Microwave Background can be used to constrain PBHs at the level of 10^{-7} [14].

The range of PBH masses from roughly 10^{17}g to 10^{26}g remains essentially unconstrained, apart from the above-mentioned narrow region around 10^{18} g. The aim of this paper is to constrain PBHs as the DM candidates in this still allowed mass range. To this end, we investigate the effect of PBHs on the evolution of compact stars – neutron stars (NSs) and white dwarfs (WDs). The main idea is as follows. PBHs may be captured by a star in the process of its formation. This leads to no observational consequences until the evolution of the star reaches the stage of a neutron star or a white dwarf. Then the accretion onto a PBH becomes sufficiently fast to destroy the compact star in a short time [15–17]. The region of PBH masses and abundances where this happens with large probability is thus excluded by observations of the

existing neutron stars and white dwarfs.

The paper is organized as follows. In Sect. II we discuss the gravitational capture of DM during the process of star formation. In Section III we derive the constraints on the fraction of PBHs in the DM from the existence of WDs and NSs. In Section IV we summarize the results and present our conclusions. Throughout the paper, we use the units $\hbar = c = 1$.

II. CAPTURE OF DARK MATTER DURING STAR FORMATION

In this section we study the capture of dark matter during the star formation process, neglecting all the DM interactions except the gravitational one. The purpose is to estimate the total amount of DM captured inside newly formed stars.

A. Star formation stages

Star formation occurs mainly in giant molecular clouds (GMCs). GMCs are dense regions of the interstellar medium composed primarily of molecular hydrogen (H_2) with typical mass $M \sim 3 \times 10^5 \, M_\odot$ and average density $\rho \sim 550 \, \mathrm{GeV \, cm^{-3}}$, which would imply a radius of 17pc in the case of a spherical shape. A GMC is usually composed of smaller overdense sub-clouds, i.e., clumps. In gravitationally bound cores inside the clumps, individual stars are formed.

The formation of stars involves different stages. The first one corresponds to the fragmentation of a GMC into gravitationally bound regions that are initially supported against gravity by a combination of rotation, magnetic and turbulent pressures [18, 19]. At some point, as the cloud core loses its magnetic and turbulent support by still poorly understood mechanisms like ambipolar diffusion [19], the growing central concentration becomes unstable to the gravitational collapse. At the initial stage of the collapse, the cloud has a uniform temperature, is rotating slowly and has an almost flat density profile in the central part. At the end of this phase an opaque protostellar object in hydrostatic equilibrium is formed at the center [20–22].

When the protostar is formed, it accretes from the surrounding disk increasing its temperature. When the central object has accumulated most of its main-sequence mass and the surrounding disk disperses, it is considered a pre-main-sequence star. The main energy source for such an object is the gravitational contraction, contrary to nuclear fusion for main sequence stars. Therefore it is evolving on a Kelvin-Helmholtz timescale $GM_*^2/(R_* L_*)$, where M_*, R_* and L_* are the mass, the radius and the luminosity of the pre-main-sequence star, respectively. This time is longer than the free fall time $(R_*^3/GM_*)^{1/2}$.

B. Adiabatic contraction

The main mechanism of the capture of DM by stars at the time of formation is the adiabatic contraction. Consider first this mechanism in general terms.

In this paper we will be interested in systems that are dominated by baryons. In this case the adiabatic contraction is easy to understand. When baryons contract losing energy by non-gravitational mechanisms, their time-dependent gravitational potential pulls the DM particles along. The DM distribution thus develops a peak centered at the baryon distribution.

If the change of the baryonic gravitational potential is slow, that is, if the characteristic time of the baryonic contraction is much larger than the free fall time $t_{\mathrm{ff}} = (G\rho_0)^{-1/2}$, where ρ_0 is the baryonic density of a cloud, the DM distribution is determined by the (approximate) conservation of the adiabatic invariant

$$\oint p \, dq = ET \qquad (1)$$

where p and q are the phase space coordinates of a DM particle of energy E and orbital period T. Moreover, the angular momentum is conserved for each DM particle as long as the potential is central. From these conserved quantities, a relation between the initial orbital radius and the final one can be derived [23–26].

Regardless of whether the contraction of DM is adiabatic or not, the phase-space density of DM has to be preserved all along the contraction process, as dictated by Liouville's theorem. For an initial Maxwellian velocity distribution of DM with the dispersion $\bar{v}$, the maximum phase space density is at zero velocity and equals [27]

$$\mathcal{Q}_{\max} = \left(\frac{3}{2\pi}\right)^{3/2} \frac{\bar{\rho}_{\mathrm{DM}}}{m_{\mathrm{DM}}^4 \bar{v}^3} \qquad (2)$$

where $\bar{\rho}_{\mathrm{DM}}$ is the space density of DM and m_{DM} is the DM mass. The effect of the adiabatic contraction is to fill all the allowed phase-space with the density close to the maximum value.

In the case of circular orbits the conservation of the angular momentum and the adiabatic invariant (1) implies the conservation of the quantity $rM(r)$, where $M(r)$ is the mass within the radius r. Suppose a baryonic cloud, which was initially a uniform sphere of radius $\bar{R}$, contracts to a compact object of a negligible size. Assuming that the DM particles move on circular orbits, the initial uniform DM density $\bar{\rho}_{\mathrm{DM}}$ is modified as follows [28]:

$$\rho_{\mathrm{DM}}(r) = \frac{1}{4} \bar{\rho}_{\mathrm{DM}} \left(\frac{\bar{R}}{r}\right)^{9/4}, \qquad (3)$$

provided the adiabatic approximation holds.

In realistic cases the orbits of DM particles are not circular. The question thus arises whether eq. (3) is a good approximation in realistic situations. An exact calculation has been performed in another limiting case of
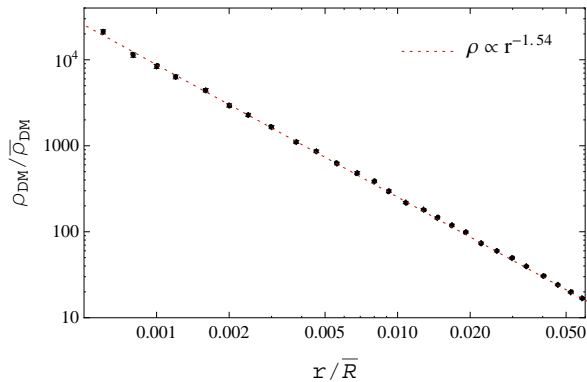
FIG. 1: DM density profile obtained from the simulation after the adiabatic formation of a star. The inner part of the profile has the slope close to $-3/2$ as expected from the Liouville's theorem for the uniform initial velocity distribution.

purely radial orbits [29, 30]. The result were found to be roughly compatible with the case of circular orbits. However, this is not a realistic case either. Another question of practical importance is the domain of validity of the adiabatic approximation. Formally, it requires the time of collapse t_c to be much longer that the free-fall time $t_{\rm ff}$. In Ref. [31] high-resolution numerical simulations have been performed and it has been shown that the adiabatic contraction may remain a good approximation, depending on the potential, even when $t_c \simeq t_{\rm ff}$.

To clarify these issues we have performed the following numerical simulation. For the baryonic distribution that is responsible for the time-varying external gravitational potential we took the sum of a uniform spherical cloud and a point mass in the center. The point mass was zero at the initial moment of time and then increased linearly with time, while the mass of the spherical part, always uniform in density, decreased in such a way that its sum with the point mass remained constant. The time t_c over which all the mass was transferred from the cloud to the central object was treated as a free parameter.

The DM particles were injected at $t = 0$ with an initial uniform distribution in position and velocity. The initial density profile was taken to be constant over the volume of the cloud to mimic the physical properties of prestellar cores. The particles were injected one by one, which corresponds to neglecting the DM contribution to the gravitational potential. Those particles which have positive total energy at $t = 0$ (and thus are not gravitationally bound to the system) were discarded; the remaining ones were evolved numerically in the time-dependent gravitational potential. At a random time $t > t_c$ the positions of these particles were sampled in order to reconstruct, after many simulations, the final density profile. As a consistency test, we have also performed an identical simulation with initial velocities of DM particles generated in such a way that the particles move on circular orbits.

In the case of circular orbits we have reproduced the

density profile (3), even for a relatively rapid change of the external potential, $t_c = 3 \, t_{\rm ff}$. In the case of random initial velocities, however, the inner profile was found to have a slope close to $-3/2$,

$$\rho_{\rm DM}(r) = \frac{1}{2}\bar{\rho}_{\rm DM}\left(\frac{\bar{R}}{r}\right)^{3/2} \qquad (4)$$

as represented in Fig. 1. These results are in agreement with Liouville's theorem, since the final DM velocity goes as $v(r) \propto r^{-1/2}$. Since random initial velocities appear to be a better approximation to realistic initial conditions than the circular ones, and because the profile (4) gives more conservative estimates, in the rest of this paper we use the profile (4).

C. DM bound to a baryonic cloud

As is clear from the above discussion, only DM gravitationally bound to a baryonic cloud is subject to the adiabatic contraction when the cloud collapses. Therefore, to set the initial conditions for the adiabatic contraction we need to estimate the amount of DM that is gravitationally bound to a cloud.

We will assume that the matter density is dominated by baryons, as is the case in the star forming regions. When the overdensity of baryons is formed, some amount of DM ends up gravitationally bound to the baryonic cloud. Consider the formation of a spherical cloud of radius R_0 and baryonic density ρ_0. Our goal is to estimate the density of DM bound to the cloud, $\rho_{\rm DM, bound}$, given the mean density of DM, $\bar{\rho}_{\rm DM}$. We will assume that originally the DM particles have the Maxwellian distribution in velocities with the dispersion $\bar{v}$,

$$dn = \bar{n}_{\rm DM}\left(\frac{3}{2\pi\bar{v}^2}\right)^{3/2} \exp\left\{\frac{-3v^2}{2\bar{v}^2}\right\} d^3v, \qquad (5)$$

where $\bar{n}_{\rm DM} = \bar{\rho}_{\rm DM}/m$, m being the mass of the DM particle. We will see that in the cases of interest the velocities of bound particles are much smaller than $\bar{v}$, and thus the precise shape of the distribution is not essential.

After the formation of a baryonic cloud, the gravitational potential felt by DM particles becomes of order

$$\phi \sim \phi_0 = 2\pi G \rho_0 R_0^2.$$

Those particles with kinetic energies smaller than ϕ_0 (equivalently, velocities $v < v_0 = \sqrt{2\phi_0}$) become gravitationally bound. Their number density is obtained by integrating eq. (5) up to $v = v_0$. Multiplying by the DM mass, one has

$$\rho_{\rm DM, bound} = \bar{\rho}_{\rm DM}\frac{4\pi}{3}\left(\frac{3|\phi_0|}{\pi\bar{v}^2}\right)^{3/2} \qquad (6)$$

$$= \bar{\rho}_{\rm DM}\frac{4\pi}{3}\left(\frac{6G\rho_0 R_0^2}{\bar{v}^2}\right)^{3/2}, \qquad (7)$$

$M_*/M_\odot$	ρ_0, GeV cm^{-3}	R_0, AU
1	10^6	4300
2	1.8×10^6	4450
3	2.4×10^6	4620
4	3.1×10^6	4710
5	3.6×10^6	4780
6	4.2×10^6	4840
7	4.8×10^6	4880
8	5.3×10^6	4930
10	6.4×10^6	5000
12	7.4×10^6	5060
15	8.8×10^6	5130

TABLE I: The parameters of prestellar cores used in the estimates.

where we have assumed $v_0 \ll \bar{v}$ and thus set the exponential to 1.

D. Globular clusters

Globular clusters (GCs) are gravitationally bound systems consisting of 10^4 to 10^7 stars with average diameters ranging from 20 to 100 pc. There are about 100 GCs known in our Galaxy. A typical GC has a baryonic mass of (a few) $\times 10^5 M_\odot$ and a core radius of $1 - 2$ pc. The age of GCs is about 8 to 13.5 Gyr [32], and as such they are the oldest surviving stellar subsystems in the galaxy, made up of the population II stars, white dwarfs, neutron stars and black holes.

There are two classes of scenarios for GC formation. According to the primordial, or "DM-dominated" one, GCs were formed by the infall of baryonic matter into the gravitational wells of the DM density peaks at redshifts $z > 10$ [33–38]. The second is the "baryon-dominated" scenario, according to which GCs were formed in predominantly baryonic processes like major mergers, hydrodynamical shocks and so on mostly in proto-galaxies that later assembled into the Milky Way [39–42]. Moreover, both mechanisms could be at work because the observed distribution of metallicity in GCs is clearly bimodal, so that metal-poor GC could be of cosmological origin, while metal-rich GCs could be formed in the course of mergers [43]. Although there is no evidence of DM presence in the GCs now [44], it was shown that it could be present at the formation time and subsequently tidally stripped due to interactions with the host galaxy [45]. We will assume in what follows that at least some of the GCs resided in DM minihaloes in the past, and concentrate on those.

The DM density in the central regions of GCs has been estimated in Ref. [46] by making use of the formalism developed in Refs. [35, 45]. The conclusion was that the present-day DM density close to the core of a GC is of order $\rho_{DM} \sim 2 \times 10^3$ GeV cm^{-3}, the estimate being rather insensitive to the original halo mass. This result is in concordance with the N-body simulations [35, 45] suggesting that the inner part of DM halos survive successive tidal interactions with the host galaxy. As has been stressed in Ref. [46], the number cited includes the effect of dynamical heating of DM by the stars comprising the cluster, which reduces the DM density. In our estimates this effect is irrelevant since we are interested in the evolution stage prior to the star formation. With no heating, the DM density in the core would be $\rho_{DM} \sim 10^4$ GeV cm^{-3}, which we adopt in what follows.

Another important parameter is the value of the DM velocity dispersion in GCs. As stars in the GC are collisionless and behave essentially as DM particles, this parameter can be extracted directly from observations. Although there is quite a bit of scatter, typical observed GCs have the velocity dispersion around $\bar{v} = 7$ km s^{-1} [47].

Let us now turn to the prestellar cores. Their typical parameters are known from observations carried out with the SCUBA instrument [48]. The dataset is well fitted by the Bonnor-Ebert profile [48] which, for our purposes, can be approximated by the flat core of radius R_0 containing the baryonic mass M_* of the future star.

Two cases will be of interest in what follows: stars with masses $1 M_\odot \leq M_* \leq 7 M_\odot$ which are typical progenitors of a WD, and supermassive stars of masses, $M_* \geq 8 M_\odot$ progenitors of NSs. In all cases the gravitational potential of the prestellar core is (much) smaller than that of the GMC, so one may use again eq. (6) to estimate the density of DM gravitationally bound to the core. We use the parameters of prestellar cores that are listed in Table I. As has been already mentioned, the formation of the prestellar cores relies on the non-gravitational energy loss mechanisms and thus is expected to be slower than the free fall.

Making use of eq. (4), one obtains the total DM mass contained in a star formed within the GCs as listed in Table II. These values were calculated with the DM density and velocity dispersion given above; for different values of these parameters the mass of the bound DM should be rescaled by the factor

$$\left(\frac{\bar{v}}{7\,\text{km/s}} \right)^{-3} \left(\frac{\bar{\rho}_{\text{DM}}}{10^4\,\text{GeV/cm}^3} \right) \qquad (8)$$

which may be different for different GCs.

III. CONSTRAINTS ON PRIMORDIAL BLACK HOLES

So far the discussion has been general and did not depend on the DM nature. Consider now specifically the case of primordial black holes. The PBHs that end up inside a star when the latter is formed start accreting and gravitationally pulling on the surrounding matter, lose their momentum and gradually sink to the center. The sinking process is slow, so that the characteristic time

$M_*/M_\odot$	$\rho_{\rm PSC}$, GeV cm^{-3}	$M_{\rm bound}$, g
1	2×10^1	4.4×10^{19}
2	5.2×10^1	2.5×10^{20}
3	9.2×10^1	7.2×10^{20}
4	1.4×10^2	1.5×10^{21}
5	1.9×10^2	2.6×10^{21}
6	2.4×10^2	4.2×10^{21}
7	3×10^2	6.2×10^{21}
8	3.6×10^2	8.7×10^{21}
10	5×10^2	1.6×10^{22}
12	6.4×10^2	2.4×10^{22}
15	8.7×10^2	4.3×10^{22}

TABLE II: Density of DM bound to the prestellar core, $\rho_{\rm PSC}$, and the total mass $M_{\rm bound}$ of DM contained in a star right after its formation in a GC with the central DM density $\rho_{DM} \sim 10^4$ GeV cm^{-3} and velocity dispersion $\bar{v} = 7$ km s^{-1} for different star masses.
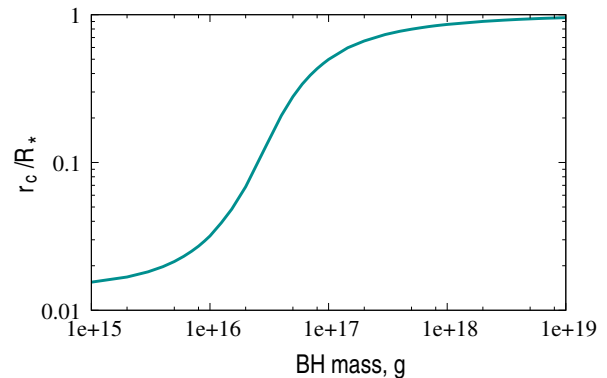

FIG. 2: The dependence of the size r_c of the collection region (the region from which the PBHs captured by the star at its formation have enough time to sink to within the radius of the future compact remnant, WD or NS) on the PBH mass, corresponding to the case of WD for $M_* = M_\odot$.

may exceed the age of the star. Because of their slow accretion and small number, the presence of BH has no observable effects on the star evolution at this stage.

When a star polluted by PBHs evolves into a compact object (WD or NS), some of the BHs get inside the compact remnant. Because of a much higher density, the accretion is now more efficient and the PBHs, if present inside the remnant, rapidly consume the latter. The observation of WDs and NSs thus implies constraints on the abundance of PBHs, which has to be such that the probability to get a PBH inside NS or WD is much less than 1.

To quantify this statement we calculate the number $N_{\rm BH}$ of BHs that would sink down to the future radius r_f of the compact remnant by the end of the star evolution and, thus, would end up inside the star remnant. If $N_{\rm BH} < 1$ no constraints arise. If $N_{\rm BH} > 1$, the maximum allowed fraction of BHs in the total amount of DM is

$$\frac{\Omega_{\rm PBH}}{\Omega_{\rm DM}} \le \frac{1}{N_{\rm BH}}. \tag{9}$$

Thus, in the range of PBH masses where $N_{\rm BH} > 1$, PBHs cannot constitute all of the DM.

The PBHs that are eventually trapped by the compact remnant initially occupy some spherical volume of radius r_c which we call the "collection region". Knowing r_c as a function of the PBH mass $m_{\rm BH}$ and the DM distribution inside the star at the time of formation allows one to calculate $N_{\rm BH}$ as follows,

$$N_{\rm BH} = M_{\rm DM}(r_c)/m_{\rm BH}, \tag{10}$$

where $M_{\rm DM}(r)$ is the DM mass contained in the radius r at the time of the star formation.

The sinking of the PBH inside the star has been considered in Ref. [30]. The dynamical friction force per unit PBH mass is given by the Eq. (16) of Ref. [30]. Multiplied by the PBH velocity, this gives the PBH energy

loss rate dE/dt. On the other hand, assuming circular orbits, dE/dt can be expressed in terms of the change of the orbit radius. Equating the two gives a closed first order differential equation for the orbit radius as a function of time, $r(t)$. We derive and solve the corresponding equation numerically in Appendix A, assuming the star model with the polytrope index $n = 3$.

Having found the dependence $r(t)$ for a given BH mass, we fix the final radius $r_f = r(t_*)$ to be the size of the compact object (NS or WD). Here t_* is the lifetime of the star. We then determine the collection radius as $r_c = r(0)$. (In practice, it is more convenient to run the evolution equations backwards in time starting from $r = r_f$.) The dependence of r_c on the BH mass is shown in Fig. 2 for $M_* = M_\odot$ and $r_f = r_{\rm WD} = 10^4$ km.

At small BH masses the dynamical friction is inefficient and the collection radius r_c is not very different from r_f. As the BH mass gets larger the friction becomes more efficient, so that r_c grows and eventually becomes close to the star radius. The transition is quite rapid; the value of $m_{\rm BH} = m_{\rm trans}$ at which it occurs can be understood analytically from the behavior of eq. (A8), see Appendix A for details. It corresponds to the smallest $m_{\rm BH}$ for which the collection radius is still close to the star size (i.e., the lifetime of the star is still sufficient for a BH to sink to $r = r_f$ starting near the surface). By an order of magnitude, it is given by

$$m_{\rm trans} \sim 4 \times 10^{17} \text{ g}$$

$$\times \left(\frac{t_*}{10 \text{ Gyr}}\right)^{-1} \left(\frac{M_*}{M_\odot}\right)^{1/2} \left(\frac{R_*}{R_\odot}\right)^{3/2}. \tag{11}$$

Note that there is no dependence on r_f because the final stages of the BH sinking are exponential, and these are the (longer) initial stages that set the overall time scale.

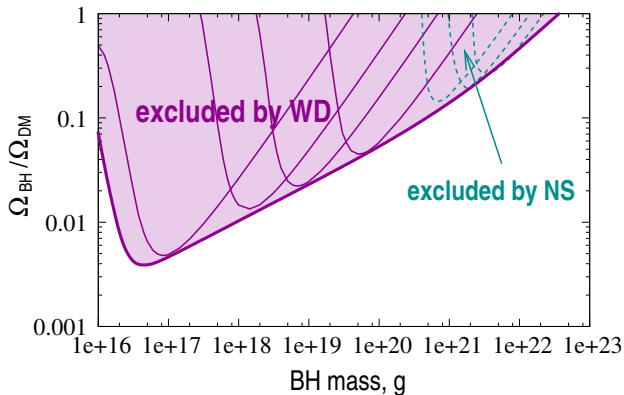The number of BHs inside the collection region $N_{\rm BH}$ can be found from the total DM mass trapped by the

FIG. 3: Constraints on the fraction $\Omega_{\rm PBH}/\Omega_{\rm DM}$. Purple shaded region is excluded by observations of WDs and NSs in the centers of globular clusters. Thin curves show the exclusions from different star masses.

star (see Table II) and the DM density profile inside the star. The DM profile inside the star after the adiabatic contraction is determined by eqs. (3) and (4) and the baryonic density, for which we assume the density profile of the polytrope $n = 3$ model. From eq. (4), the DM and baryonic masses are related as follows,

$$M_{\rm DM}(r) = M_{\rm bound} \left(\frac{M(r)r^3}{M_* R_*^3} \right)^{1/2}, \qquad (12)$$

where $M(r)$ and $M_{\rm DM}(r)$ are the baryonic and DM mass within the radius r, respectively. The number of BH within r_c is then given by eq. (10).

The resulting constraints on the fraction of PBHs in the total amount of DM are shown in Fig. 3. Purple shading shows the region excluded by the observations of WDs and NSs in the globular clusters. Thin curves show the exclusion regions resulting from different star masses. One can see that the constraints from WDs and NSs complement each other and together cover the range of masses from 10^{16} g to 3×10^{22} g.

The shape of the excluded regions is similar in all cases shown in Fig. 3. It can be understood from the mass dependence of the collection radius r_c, Fig. 2, as follows. At large PBH masses the size of the collection region is close to the star size, so that $M_{\rm DM}(r_c) \simeq M_{\rm bound}$ and the maximum PBH fraction $\Omega_{\rm PBH}/\Omega_{\rm DM}$ scales like $m_{\rm BH}$, i.e., the constraints improve at smaller masses. However, at some point around $m_{\rm BH} \sim m_{\rm trans}$ the collection radius r_c decreases (cf. Fig. 2) and the constraints get relaxed very rapidly.

IV. CONCLUSIONS

We have derived the constraints on the abundance of PBH from observations of the existing WDs and NSs. The origin of these constraints is as follows. If PBHs were present at the time of star formation, i.e., at $z \lesssim 10$, they

would pollute the newly-formed stars and, after sinking to the center, would end up in the compact remnant resulting from the star evolution (WD or NS). Once inside the remnant, PBHs would rapidly destroy it by accretion. Mere observations of WDs and NSs, therefore, impose constraints on the abundance of PBHs.

We have found that the most stringent constraints come from observations of WDs and NSs in globular clusters. WDs and NSs are sensitive to the mass ranges $10^{16}\,{\rm g} \lesssim m_{\rm BH} \lesssim 10^{21}\,{\rm g}$ and $10^{21}\,{\rm g} \lesssim m_{\rm BH} \lesssim 3 \times 10^{22}\,{\rm g}$, respectively, thus complementing each other. Everywhere in this mass range the PBHs are excluded as comprising all of the DM. The best constraint on the PBH fraction $\Omega_{\rm PBH}/\Omega_{\rm DM} \lesssim 10^{-2}$ was found for $m_{\rm BH}$ in the range $10^{17}\,{\rm g} - 10^{18}\,{\rm g}$.

The constraints derived from the globular clusters are based on the assumption that at least some of those were formed in a primordial DM-dominated environment. As a word of warning, it should be noted that this issue is still debated in the literature. For instance, observations of a low-metallicity cluster NGC 2419 [49, 50] seem to indicate that its mass-to-light ratio is in a good agreement with what is expected for a pure baryonic system. However, NGC 2419 has a number of extreme properties [51–53] that make the globular cluster nature of this object questionable. In addition, high-resolutions N-body simulations [35, 45] indicate that the mass-to-light ratio may not be sensitive to the presence of the DM component in GCs.

In order to derive the constraints on the PBH abundance we have investigated the baryonic contraction of the DM during the star formation process. In particular, we have calculated numerically the resulting DM profile and found the slope close to $-3/2$. We also estimated the total amount of DM that is trapped inside the star at the time of its formation. This part of our results is not specific to any particular form of the DM.

Appendix A: Sinking of BH in the star

Here we consider the energy loss by a BH that is orbiting inside a star gradually sinking to the center. The

star is assumed to have an r-dependent density $\rho(r)$ and temperature $T(r)$, and the mass $M(r)$ enclosed inside the radius r. Our purpose is to derive the equation that governs the evolution of the BH orbit due to the dynamical friction, assuming the orbit is circular and changes slowly. The question of dynamical friction was considered in a general context , e.g., in Refs.[54, 55].

The BH moving through a star experiences a dynamical friction force [55] that can be written as follows,

$$\frac{\mathbf{f}}{m_{\mathrm{BH}}} = -\gamma(v)\mathbf{v}, \tag{A1}$$

where

$$\gamma(v) = 4\pi G^2 \rho(r) m_{\mathrm{BH}} \ln(\Lambda) \frac{F(X)}{v^3},$$

$$F(X) = \mathrm{erf}(X) - 2X\exp(-X^2)/\sqrt{\pi}, \tag{A2}$$

$$X = v/(\sqrt{2}\sigma),$$

$\rho(r)$ is the density of the baryonic gas comprising the star, σ is the velocity dispersion of the particles $\sigma = \sqrt{T/m}$ with temperature T and mean molecular weight m ($m \simeq 1.6$ GeV for a main sequence star), and $\ln(\Lambda) \simeq \ln(M_*/m_{\mathrm{BH}}) \simeq 30$ is the Coulomb logarithm [55]. Multiplying Eq. (A1) by $\mathbf{v}$ gives the total BH energy loss rate per unit mass, $dE/dt = -\gamma(v)v^2$.

Making use of the relation

$$v^2 = GM(r)/r, \tag{A3}$$

the same energy loss rate can be expressed through the change of the radius r of the BH orbit,

$$\frac{dE}{dt} = \frac{d}{dt}\left(\frac{1}{2}v^2 + U(r)\right) = \frac{dr}{dt}\frac{v^2}{2r}\left\{\frac{4\pi r^3}{M(r)}\rho(r) + 1\right\}, \tag{A4}$$

where $U(r)$ is the gravitational potential. Equating the two quantities and simplifying by v^2 one gets

$$\frac{dr}{dt}\frac{1}{2r}\left\{\frac{4\pi r^3}{M(r)}\rho(r) + 1\right\} = -\gamma(v). \tag{A5}$$

By virtue of eq. (A3), this is a closed differential equation for the BH orbit radius $r(t)$ as a function of time. Note that this equation is not equivalent to eq. (24) of Ref. [30] because the contribution of the gravitational potential (the term $U(r)$ in eq. (A4)) has been missed there.

Let us rewrite this equation in the form convenient for the numerical solution. Define the dimensionless quantities

$$\begin{aligned} x &= r/R_*, \\ \tau &= t/t_0, \\ \tilde{\rho}(r) &= \rho(r)/\rho(0), \\ \tilde{M}(r) &= M(r)/M_*, \\ \tilde{T}(r) &= T(r)/T(0), \end{aligned}$$

where

$$t_0 = \frac{M_*^{3/2}}{2\pi\sqrt{G}\rho(0)m_{\mathrm{BH}}R_*^{3/2}\ln\Lambda} \tag{A6}$$

$$\simeq 4.2 \times 10^3 \,\mathrm{yr}\left(\frac{m_{\mathrm{BH}}}{10^{22}\mathrm{g}}\right)^{-1}\left(\frac{M_*}{M_\odot}\right)^{1/2}\left(\frac{R_*}{R_\odot}\right)^{3/2}. \tag{A7}$$

The profiles $\tilde{\rho}(r)$ and $\tilde{T}(r)$ are determined by the star model. The normalization parameters $\rho(0)$, $T(0)$, M_* and R_* are not independent. They obey the following two relations,

$$\begin{aligned} \frac{GM_*m}{R_*T(0)} &= 1.17 \\ \frac{\rho(0)R_*^3}{M_*} &= 12.9, \end{aligned}$$

where, as before, m is the mean molecular weight. The scaling in eq. (A7) takes into account these relations.

In terms of the dimensionless quantities, Eq. (A5) becomes

$$\frac{dx}{d\tau} = -\frac{x^{5/2}\tilde{\rho}(x)}{f(x)\tilde{M}^{3/2}(x)}F(X). \tag{A8}$$

Here we have introduced the function

$$f(x) = \frac{1}{4}\left\{4\pi\frac{r^3\rho(r)}{M(r)} + 1\right\} = \frac{1}{4}\left\{163\frac{x^3\tilde{\rho}(x)}{\tilde{M}(x)} + 1\right\}$$

which varies between 1 in the star center $x = 0$ and $1/4$ at the star surface $x = 1$. The variable X is in turn a function of x which can be expressed as follows,

$$X = \left(\frac{GmM(r)}{2rT(r)}\right)^{1/2} = 0.765\left(\frac{\tilde{M}(x)}{x\tilde{T}(x)}\right)^{1/2},$$

while the function $F(X)$ is defined in Eq. (A2). At small values of X this function behaves as $4X^3/(3\sqrt{\pi})$; at large X it asymptotes to 1.

A useful analytical insight into behavior of the eq. (A8) can be obtained by considering two limiting cases. At small values of x such that the parameters of the star can still be approximated by their core values one has

$$X \simeq 5.62x.$$

At small x such that $X \ll 1$ eq. (A8) becomes

$$\frac{dx}{d\tau} = -0.337x,$$

whose solution is $x(t) = \exp(-0.337t/t_0)$ with t_0 given by eq. (A6). In this regime, valid for the final approach by a sinking BH of the radius r_f (the radius of a future compact object), the characteristic time scale is

$$(\Delta t)_2 \simeq 3\ln(r_0/r_f)\,t_0,$$

where r_0 is some initial radius.

At moderately small x such that $X \gtrsim 1$ eq. (A6) takes the form

$$\frac{dx}{d\tau} = -\frac{1}{397\,x^2},$$

which gives the evolution time $(\Delta t)_1$ from x_1 to x_2

$$(\Delta t)_1 = 132\,t_0(x_1^3 - x_2^3) \simeq 10^2 \times t_0,$$

where we have set $x_1^3 \sim 1$ and neglected x_2^3. We see that this first stage is typically longer than the second, $(\Delta t)_1 > (\Delta t)_2$. Equating $(\Delta t)_1$ to the lifetime of the star t_* and making use of eq. (A6) leads to the estimate (11).

[1] G. Bertone, D. Hooper, and J. Silk, Phys.Rept. **405**, 279 (2005), hep-ph/0404175.
[2] L. Bergstrom (2012), 1205.4882.
[3] E. Komatsu et al. (WMAP Collaboration), Astrophys.J.Suppl. **192**, 18 (2011), 1001.4538.
[4] S. Hawking, Mon.Not.Roy.Astron.Soc. **152**, 75 (1971).
[5] A. Dolgov and J. Silk, Phys.Rev. **D47**, 4244 (1993).
[6] A. M. Green and A. R. Liddle, Phys.Rev. **D60**, 063509 (1999), astro-ph/9901268.
[7] S. Hawking, Nature **248**, 30 (1974).
[8] D. N. Page and S. Hawking, Astrophys.J. **206**, 1 (1976).
[9] P. Sreekumar et al. (EGRET Collaboration), Astrophys.J. **494**, 523 (1998), astro-ph/9709257.
[10] B.J. Carr, K. Kohri, Y. Sendouda, and J. Yokoyama, Phys.Rev. **D81**, 104019 (2010), astro-ph/0912.5297.
[11] A. Gould, Astrophys. J. Lett. **386**, L5 (1992).
[12] A. Barnacka, J.-F. Glicenstein, and R. Moderski, Phys. Rev. D **86**, 043001 (2012), 1204.2056.
[13] P. Tisserand et al. (EROS-2 Collaboration), Astron.Astrophys. **469**, 387 (2007), astro-ph/0607207.
[14] M. Ricotti, J. P. Ostriker, and K. J. Mack (2007), 0709.0524.
[15] C. Kouvaris and P. Tinyakov, Phys.Rev.Lett. **107**, 091301 (2011), 1104.0382.
[16] C. Kouvaris, Phys.Rev.Lett. **108**, 191301 (2012), 1111.4364.
[17] C. Kouvaris and P. Tinyakov, Phys.Rev. **D83**, 083512 (2011), 1012.2039.
[18] T. C. Mouschovias and S. A. Morton, Astrophys. J. **371**, 296 (1991).
[19] F. H. Shu, F. C. Adams, and S. Lizano, ARA&A **25**, 23 (1987).
[20] R. B. Larson, Mon. Not. R. Astron. Soc. **145**, 271 (1969).
[21] A. P. Boss and H. W. Yorke, Astrophys. J. Lett. **439**, L55 (1995).
[22] M. R. Bate, Astrophys. J. Lett. **508**, L95 (1998), astro-ph/9810397.
[23] G. R. Blumenthal, S. Faber, R. Flores, and J. R. Primack, Astrophys.J. **301**, 27 (1986).
[24] O. Y. Gnedin, A. V. Kravtsov, A. A. Klypin, and D. Nagai, Astrophys.J. **616**, 16 (2004), astro-ph/0406247.
[25] J. A. Sellwood and S. S. McGaugh, Astrophys.J. **634**, 70 (2005), astro-ph/0507589.
[26] E. V. Derishev and A. A. Belyanin, Astron. Astrophys. **343**, 1 (1999).
[27] S. Tremaine and J.E. Gunn, Phys.Rev.Lett. **42**, 407 (1979).
[28] G. Steigman, C. L. Sarazin, H. Quintana, and J. Faulkner, Astron. J. **83**, 1050 (1978).
[29] D. Spolyar, K. Freese, and P. Gondolo, Phys.Rev.Lett. **100**, 051101 (2008), astro-ph/0705.0521.
[30] C. Bambi, D. Spolyar, A. D. Dolgov, K. Freese, and M. Volonteri, Mon.Not.Roy.Astron.Soc. **399**, 1347 (2009), astro-ph/0812.0585.
[31] R. Jesseit, T. Naab, and A. Burkert, Astrophys. J. Lett. **571**, L89 (2002), astro-ph/0204164.
[32] A. Dotter, A. Sarajedini, J. Anderson, A. Aparicio, L. R. Bedin, B. Chaboyer, S. Majewski, A. Marín-Franch, A. Milone, N. Paust, et al., Astrophys. J. **708**, 698 (2010), 0911.2469.
[33] P. J. E. Peebles, Astrophys. J. **277**, 470 (1984).
[34] V. Bromm and C. J. Clarke, Astrophys. J. Lett. **566**, L1 (2002), arXiv:astro-ph/0201066.
[35] S. Mashchenko and A. Sills, Astrophys. J. **619**, 243 (2005), arXiv:astro-ph/0409605.
[36] B. Moore, J. Diemand, P. Madau, M. Zemp, and J. Stadel, Mon. Not. R. Astron. Soc. **368**, 563 (2006), arXiv:astro-ph/0510370.
[37] A. C. Boley, G. Lake, J. Read, and R. Teyssier, Astrophys. J. Lett. **706**, L192 (2009), 0908.1254.
[38] B. F. Griffen, M. J. Drinkwater, P. A. Thomas, J. C. Helly, and K. A. Pimbblet, Mon. Not. R. Astron. Soc. **405**, 375 (2010), 0910.0310.
[39] S. M. Fall and M. J. Rees, Astrophys. J. **298**, 18 (1985).
[40] K. M. Ashman and S. E. Zepf, Astrophys. J. **384**, 50 (1992).
[41] A. V. Kravtsov and O. Y. Gnedin, Astrophys. J. **623**, 650 (2005), arXiv:astro-ph/0305199.
[42] A. L. Muratov and O. Y. Gnedin, Astrophys. J. **718**, 1266 (2010), 1002.1325.
[43] J. P. Brodie and J. Strader, ARA&A **44**, 193 (2006), arXiv:astro-ph/0602601.
[44] B. Moore, Astrophys. J. Lett. **461**, L13 (1996), arXiv:astro-ph/9511147.
[45] S. Mashchenko and A. Sills, Astrophys. J. **619**, 258 (2005), arXiv:astro-ph/0409606.
[46] G. Bertone and M. Fairbairn, Phys.Rev. **D77**, 043515 (2008), 0709.1485.
[47] W. E. Harris, Astron. J. **112**, 1487 (1996).
[48] J. M. Kirk, D. Ward-Thompson, and P. Andre, Mon.Not.Roy.Astron.Soc. **360**, 1506 (2005), astro-ph/0505190.
[49] H. Baumgardt, P. Côté, M. Hilker, M. Rejkuba, S. Mieske, S. G. Djorgovski, and P. Stetson, Mon. Not. R. Astron. Soc. **396**, 2051 (2009), 0904.3329.
[50] C. Conroy, A. Loeb, and D. Spergel, Astrophys.J. **741**, 72 (2011), 1010.5783.
[51] A. D. Mackey and S. van den Bergh, Mon. Not. R. As-

tron. Soc. **360**, 631 (2005), arXiv:astro-ph/0504142.

[52] J. G. Cohen and E. N. Kirby, ArXiv e-prints (2012), 1209.2705.

[53] J. G. Cohen, E. N. Kirby, J. D. Simon, and M. Geha, Astrophys. J. **725**, 288 (2010), 1010.0031.

[54] S. Chandrasekhar, Reviews of Modern Physics **21**, 383 (1949).

[55] J. Binney and S. Tremaine, *Galactic dynamics* (1987).